

## Master Formula Approach to $\gamma\gamma \rightarrow \pi\pi$ processes

S. Chernyshev and I. Zahed

*Department of Physics, SUNY, Stony Brook, New York 11794-3800*

### Abstract

We analyze the  $\gamma\gamma \rightarrow \pi^0\pi^0$  and  $\gamma\gamma \rightarrow \pi^+\pi^-$  reactions using the master formula approach to chiral symmetry breaking. The pertinent vacuum correlators are estimated at tree level, and the results are compared with one- and two-loop chiral perturbation theory. The Compton scattering amplitude and the pion polarizabilities are also discussed.

## 1. Introduction

At low energy, the fusion process  $\gamma\gamma \rightarrow \pi^0\pi^0$  is directly proportional to pion loops. One-loop chiral perturbation theory [1, 2] yields a result that is at odds with the data [3] by several standard deviations even at threshold, suggesting important correlations in the scalar-isoscalar channel. Two-loop chiral perturbation [4] does better, with the help of few parameters that are fixed by resonance saturation. The data can also be fit using constraints from dispersion theory [5], chiral perturbation theory [6] and effective models [7].

In the present work, we will provide an analysis of  $\gamma\gamma \rightarrow \pi^+\pi^-$  and  $\gamma\gamma \rightarrow \pi^0\pi^0$ , reactions from the point of view of the master formula approach to chiral symmetry breaking [8]. In this approach, chiral symmetry and unitarity are enforced without recourse to an expansion scheme. The result is a fusion amplitude that is expressed as the sum of two vacuum correlation functions. These correlation functions are amenable to power counting, lattice simulations or model calculations.

Using power counting in  $1/f_\pi$ , the various correlation functions may be analyzed to one-loop. The results have been discussed in [8], and are overall similar to one-loop chiral perturbation theory. The effects of correlations can be either addressed by expanding further the correlators in  $1/f_\pi$  or saturating them with physical states. In this paper, we will choose the latter route, since the former is likely to be similar to two-loop chiral perturbation theory. In section 2, we present our calculations. In section 3, we discuss the fusion cross sections and compare them with one- and two-loop chiral perturbation theory. In section 4, the Compton amplitudes are derived by crossing and compared to one- and two-loop chiral perturbation theory. Our concluding remarks are presented in section 5.

## 2. Calculation

Let us consider the reaction  $\gamma^c(q_1) \gamma^d(q_2) \rightarrow \pi^a(k_1) \pi^b(k_2)$  in the gauge where the photon polarizabilities satisfy the condition  $\epsilon_\mu(q_i)q_j^\mu = 0$ , with  $i, j = 1, 2$ . Then,  $\epsilon_1 \cdot k_1 = -\epsilon_1 \cdot k_2$ . Let us define the Mandelstam variables to be

$$\begin{aligned} s &= (q_1 + q_2)^2 = 2q_1 \cdot q_2 \\ t &= (q_1 - k_1)^2 = m_\pi^2 - 2q_1 \cdot k_1 \\ u &= (q_1 - k_2)^2 = m_\pi^2 - 2q_1 \cdot k_2 \end{aligned} \quad (1)$$

Throughout  $q_1^2 = q_2^2 = 0$  and  $p_1^2 = p_2^2 = m_\pi^2$ . The master formula approach to the  $\gamma\gamma \rightarrow \pi\pi$  reaction reads [8]

$$\begin{aligned} \mathcal{T}^{abcd}(s, t, u) = & + i \epsilon_1 \cdot \epsilon_2 \left( \epsilon^{bce} \epsilon^{eda} + \epsilon^{bde} \epsilon^{eca} \right) \\ & + 4i \epsilon_1 \cdot k_1 \epsilon_2 \cdot k_2 \left( \frac{1}{u - m_\pi^2} \epsilon^{bcf} \epsilon^{fda} + \frac{1}{t - m_\pi^2} \epsilon^{bdf} \epsilon^{fca} \right) \\ & + \frac{1}{2f_\pi^2} \epsilon_1^\mu \epsilon_2^\nu (k_2 - k_1)^\beta \epsilon^{abg} \int d^4y d^4z e^{-iq_1 \cdot y - iq_2 \cdot z} \\ & \times \langle 0 | T^* \left( \mathbf{V}_\mu^c(y) \mathbf{V}_\nu^d(z) \mathbf{V}_\beta^g(0) \right) | 0 \rangle_{conn} \\ & + \frac{1}{f_\pi^2} \epsilon_1^\mu \epsilon_2^\nu k_1^\alpha k_2^\beta \int d^4y d^4z_1 d^4z_2 e^{-iq_1 \cdot y + ik_1 \cdot z_1 + ik_2 \cdot z_2} \\ & \times \langle 0 | T^* \left( \mathbf{j}_{A\alpha}^a(z_1) \mathbf{j}_{A\beta}^b(z_2) \mathbf{V}_\mu^c(y) \mathbf{V}_\nu^d(0) \right) | 0 \rangle_{conn} \\ & - \frac{i}{f_\pi} m_\pi^2 \delta^{ab} \epsilon_1^\mu \epsilon_2^\nu \int d^4y d^4z e^{-iq_1 \cdot y - iq_2 \cdot z} \\ & \times \langle 0 | T^* \left( \mathbf{V}_\mu^c(y) \mathbf{V}_\nu^d(z) \hat{\sigma}(0) \right) | 0 \rangle_{conn} \end{aligned} \quad (2)$$

The first and second lines in (2) are the seagull and Born terms respectively.  $\mathbf{V}_\mu^a$  is the vector current in QCD and  $\mathbf{j}_{A\alpha}^a$  is the one-pion reduced axial-current in QCD. The scalar density  $\hat{\sigma}$  is defined by

$$\hat{\sigma} = -f_\pi - \frac{\hat{m}}{f_\pi m_\pi^2} \bar{q}q \quad (3)$$

For more details on (2) we refer to [8]. The dominant contributions to (2) are shown in Fig. 1. Note, that for  $c = d = 3$  the correlation function  $\mathbf{VVV}$  does not contribute. For the fusion of two real photons, only the correlation functions  $\mathbf{jjVV}$  and  $\mathbf{VV}\hat{\sigma}$  contribute. Their contribution to one-loop was analyzed in [8].

In general, the correlation functions  $\mathbf{jjVV}$  and  $\mathbf{VV}\hat{\sigma}$  diverge at short distances, and require subtractions. Naive power counting shows that only one-subtraction is needed for each of the correlation function. The subtraction constants in  $\mathbf{jjVV}$  and  $\mathbf{VV}\hat{\sigma}$  will be set to zero because of charge-conservation in the crossed channel. Having said this, it is now equivalent to trade the  $T^*$ -product in (2) by the  $T$ -product, and saturate the time-ordered correlators with physical states at tree level. Using

$$\langle 0 | \mathbf{V}_\mu^a(x) | \rho^b(p) \rangle \sim \delta^{ab} \epsilon_\mu^V(p) f_\rho m_\rho e^{-ip \cdot x} \quad (4)$$

the result reads

$$\begin{aligned} V_{\text{tree}}^{ab} = & + \epsilon^1 \cdot \epsilon^2 \frac{m_\rho^2 f_\rho^2}{f_\pi^2} \frac{i}{q_1^2 - m_\rho^2} k_1^\alpha \langle \rho^3(q_1) | \mathbf{j}_{A\alpha}^a | A^f(Q) \rangle \\ & \times \left( \frac{i}{t - m_A^2} + \frac{i}{u - m_A^2} \right) k_2^\beta \langle A^f(Q) | \mathbf{j}_{A\beta}^b | \rho^3(q_2) \rangle \frac{i}{q_2^2 - m_\rho^2} \\ & - \epsilon^1 \cdot \epsilon^2 \frac{m_\rho^2 f_\rho^2}{f_\pi} m_\pi^2 \delta^{ab} \frac{i}{q_1^2 - m_\rho^2} v_{\sigma\rho\rho}(s) \\ & \times \frac{i}{s - m_\sigma^2} \langle \sigma(q_2) | \hat{\sigma} | 0 \rangle \frac{i}{q_2^2 - m_\rho^2} \end{aligned} \quad (5)$$

where the propagators carry the Feynman prescription. The state  $|A^f(Q)\rangle$  refers to an axial vector particle of mass  $m_A$  with momentum  $Q = q_1 - k_1$  in the t-channel, and  $Q = q_1 - k_2$  in the u-channel, while the state  $|\sigma(q)\rangle$  refers to a scalar particle of mass  $m_\sigma$ . These particles will be assigned specific widths in the discussion to follow.

In Fig. 2, we show additional tree level contributions to  $\mathbf{jjVV}$ . However, these contributions to the amplitude are two orders of magnitude down compared to the ones shown

in Fig. 1, and will be ignored <sup>1</sup>. Indeed, the contributions to (2) from Fig. 2, are just through the longitudinal parts  $k_1 \cdot \mathbf{j}_A k_2 \cdot \mathbf{j}_A \sim (m_\pi^2/m_A^2)^2$ . Thus a factor  $m_\pi^2/m_A^2 \sim 10^{-2}$  down compared to the dominant parts in (5), following from Fig.1. We also note that in chiral models with vector mesons [9, 10], there is usually no  $\pi A_1$ -mixing, and so these contributions are just zero in the fusion amplitude.

The matrix elements and vertices appearing in (5) are not known. Assuming that they are analytic in the invariant momenta, we will only retain their leading behaviour at low energy. For the scalar, we will use  $\langle 0|\bar{q}q|\sigma(q)\rangle = \lambda_\sigma^2 \sim m_\sigma^2$  as suggested by instanton simulations [11], and confirmed by our fit (see below). For the transition matrix element of the axial-vector current between the  $\rho$  and the  $a_1$ , we will use the general decomposition

$$\langle \rho^3(q_1)|\mathbf{j}_{A\alpha}^a|A^f(q_1 - k_1)\rangle \sim i\epsilon^{3af} \left[ k_1^\alpha F_1 \epsilon^A \cdot \epsilon^V + \epsilon_\alpha^V F_2 k_1 \cdot \epsilon^A + \epsilon_\alpha^A F_3 k_1 \cdot \epsilon^V \right] \quad (6)$$

where  $\epsilon^A$  and  $\epsilon^V$  stand for the vector and the axial polarizations respectively. Charge-conservation in the crossed (Compton) channel requires that  $F_1 = 0$  and  $F_2 = -F_3 = F_A$ . For simplicity, we will set  $F_A$  to a constant. Finally, for the  $\rho\rho\sigma$  vertex, we choose

$$v_{\sigma\rho\rho}(s) = i\gamma_{\rho\rho\sigma} \frac{s}{m_\sigma^2} \quad (7)$$

A constant contribution to (7) violates charge neutrality of the  $\pi^0$ , since it gives a non-zero charge to  $\pi^0$  in the Compton amplitude by crossing. Order  $\mathcal{O}(s^2)$  have been ignored for simplicity.

Using the above parametrizations for the matrix elements, we obtain for the fusion amplitude

$$V_{\text{tree}}^{ab} = i\epsilon^1 \cdot \epsilon^2 \delta^{ab} \frac{f_\rho^2 m_\pi^2}{f_\pi^2 m_\rho^2} \left\{ F_A^2 \frac{s}{m_\pi^2} \frac{g(s, t, u)}{u - m_A^2} + \frac{\hat{m}\gamma_{\rho\rho\sigma}}{m_\pi^2} \frac{s}{s - m_\sigma^2} \right\} \quad (8)$$

---

<sup>1</sup>Note that if we were to express the A-propagator in a Landau-like gauge, these contributions will just drop from the amplitude because of transversality.

with

$$g(s, t, u) = \frac{(4m_\pi^2 - s)}{2} - \frac{(m_\pi^2 + u)^2}{4m_A^2} + \frac{(m_\pi^2 - t)(m_\pi^2 - u) - sm_\pi^2}{4m_\rho^2} + \frac{s(m_\pi^2 + u)^2}{16m_\rho^2 m_A^2} \quad (9)$$

The parameters in (9) are  $F_A$  and  $\gamma_{\rho\rho\sigma}$ . The various masses, decay widths and decay constants  $f_A, f_\rho$ , are fixed by experiment.

### 3. Cross sections

• For the neutral fusion process  $\gamma\gamma \rightarrow \pi^0\pi^0$  the first (seagull), second (Born) and third terms in (2) drop and the amplitude reads

$$\mathcal{T}_{\gamma\gamma \rightarrow \pi^0\pi^0} = ie^2 \epsilon_1 \cdot \epsilon_2 \frac{f_\rho^2 m_\pi^2}{f_\pi^2 m_\rho^2} \frac{\hat{m} \gamma_{\rho\rho\sigma}}{m_\pi^2} \frac{s}{s - m_\sigma^2} \quad (10)$$

Let  $\Gamma_\sigma$  be the momentum dependent width of the scalar particle [12],

$$\Gamma_\sigma(q^2) = \Gamma_1 \left( \frac{1 - 4m_\pi^2/q^2}{1 - 4m_\pi^2/m_\sigma^2} \right)^{1/2} \quad (11)$$

The differential cross section for the neutral fusion process receives contribution only from the  $\mathbf{V}\mathbf{V}\hat{\sigma}$  in the form

$$\left( \frac{d\sigma}{d\Omega} \right)_{\gamma\gamma \rightarrow \pi^0\pi^0} = \frac{\alpha^2 \beta_V}{4s} \left| \frac{m_\pi}{2\alpha} \alpha_\pi^0(s) s \right|^2 \quad (12)$$

with a neutral polarization function for the fusion process given by

$$\alpha_\pi^0(s) = \frac{\alpha m_\pi f_\rho^2}{f_\pi^2 m_\rho^2} \frac{\hat{m} \gamma_{\rho\rho\sigma}}{m_\pi^2} \frac{1}{s - m_\sigma^2 + im_\sigma \Gamma_\sigma} \quad (13)$$

Here  $\beta_V = \sqrt{1 - 4m_\pi^2/s}$  is the pion velocity in the CM frame.

Using  $m_\sigma = 500\text{MeV}$  and  $\Gamma_1 = 550\text{MeV}$ , an overall fit to the total cross section as shown in Fig. 2, implies that

$$\gamma_{\rho\rho\sigma} \simeq 6.1 \frac{m_\pi^2}{\hat{m}} \quad (14)$$

Small changes in the scalar parameters are possible. Large changes, however, will upset the fit. This implies the presence of a low mass scalar-isoscalar contribution in the neutral fusion process, albeit with a large width.

- For the charged fusion process  $\gamma\gamma \rightarrow \pi^+\pi^-$  the seagull and Born terms in (2) contribute, while the third term  $\mathbf{VVV}$  drops. The amplitude reads

$$\begin{aligned} \mathcal{T}_{\gamma\gamma \rightarrow \pi^+\pi^-} = & -4ie^2 \epsilon_1 \cdot k_1 \epsilon_2 \cdot k_2 \left( \frac{1}{t - m_\pi^2} + \frac{1}{u - m_\pi^2} \right) \\ & - 2ie^2 \epsilon_1 \cdot \epsilon_2 \left( 1 - \frac{f_\rho^2}{2f_\pi^2} \frac{sF_A^2}{m_\rho^2} \frac{g(s, t, u)}{u - m_A^2} - \frac{f_\rho^2 m_\pi^2}{2f_\pi^2 m_\rho^2} \frac{\hat{m}\gamma_{\rho\rho\sigma}}{m_\pi^2} \frac{s}{s - m_\sigma^2} \right) \end{aligned} \quad (15)$$

The differential cross section for the charged fusion process can be written in the following form

$$\left( \frac{d\sigma}{d\Omega} \right)_{\gamma\gamma \rightarrow \pi^+\pi^-} = \frac{\alpha^2 \beta_V}{4s} \left( +|1 + \frac{m_\pi}{2\alpha} \alpha_\pi^\pm(s)s|^2 + |\mathbf{B} + \frac{m_\pi}{2\alpha} \alpha_\pi^\pm(s)s|^2 \right) \quad (16)$$

with a charged polarization function given by

$$\alpha_\pi^\pm(s) = -\frac{\alpha m_\pi f_\rho^2}{f_\pi^2 m_\rho^2} \left( \frac{m_\pi^2}{s} - 1 \right) \left( \frac{F_A^2}{m_\pi^2} \frac{g(s, t, u)}{u - m_A^2} + \frac{\hat{m}\gamma_{\rho\rho\sigma}}{m_\pi^2} \frac{1}{s - m_\sigma^2} \right) \quad (17)$$

and a Born contribution

$$\mathbf{B} = -1 + \frac{2sm_\pi^2}{(t - m_\pi^2)(u - m_\pi^2)} \quad (18)$$

For  $F_A = 1$  the contribution to the Born term is small, and the differential cross section is in overall agreement with the data as shown in Fig. 3.

#### 4. Compton Scattering

- For  $\gamma(q_1) \pi^0(k_1) \rightarrow \gamma(q_2) \pi^0(k_2)$  we have by crossing  $s \leftrightarrow t$

$$\left( \frac{d\sigma}{d\Omega} \right)_{\gamma\pi^0 \rightarrow \gamma\pi^0} = \frac{m_\pi^2}{4s} \left| \frac{\alpha m_\pi}{2} \frac{f_\rho^2}{f_\pi^2 m_\rho^2} \frac{\hat{m}\gamma_{\rho\rho\sigma}}{m_\pi^2} \frac{t}{t - m_\sigma^2 + im_\sigma\Gamma_\sigma} \right|^2 \quad (19)$$

which yields the following neutral pion polarizability

$$\alpha_\pi^0(0) = -\frac{\alpha m_\pi}{2} \frac{f_\rho^2}{f_\pi^2 m_\rho^2} \frac{\hat{m} \gamma_{\rho\rho\sigma}}{m_\pi^2} \frac{1}{m_\sigma^2 + \Gamma_\sigma^2} \simeq -2.2 \cdot 10^{-4} \text{ fm}^3 \quad (20)$$

where we used  $m_\pi = 135$  MeV,  $f_\pi = 93$  MeV and  $f_\rho = 144$  MeV. This result is to be compared with the result of  $-0.49 \cdot 10^{-4} \text{ fm}^3$  following from one-loop chiral perturbation theory [13], and the data  $\alpha_\pi^0(\text{exp}) = (0.69 \pm 0.07 \pm 0.04) \cdot 10^{-4} \text{ fm}^3$  [14] and  $\alpha_\pi^0(\text{exp}) = (0.8 \pm 2.0) \cdot 10^{-4} \text{ fm}^3$  [15]. The Compton scattering amplitude as a function of  $\sqrt{s}$  is shown in Fig. 4. (solid line), in comparison with one-loop (dot-dashed) and two-loop (dashed) chiral perturbation theory [4].

- The differential cross section for the charged Compton process  $\gamma(q_1) \pi^\pm(k_1) \rightarrow \gamma(q_2) \pi^\pm(k_2)$  is

$$\left( \frac{d\sigma}{d\Omega} \right)_{\gamma\pi^\pm \rightarrow \gamma\pi^\pm} = \frac{\alpha^2}{2s} \left( \left| 1 + \frac{m_\pi}{2\alpha} \alpha_\pi^\pm(t)t \right|^2 + \left| \overline{\mathbf{B}} + \frac{m_\pi}{2\alpha} \alpha_\pi^\pm(t)t \right|^2 \right) \quad (21)$$

with a charged polarization function for the charged Compton process given by (17) with  $s \rightarrow t$ , and a Born contribution

$$\overline{\mathbf{B}} = -1 + \frac{2tm_\pi^2}{(s - m_\pi^2)(u - m_\pi^2)} \quad (22)$$

From (21) we read the charged pion polarizability

$$\begin{aligned} \alpha_\pi^\pm(0) &= -\frac{\alpha m_\pi}{2} \frac{f_\rho^2}{f_\pi^2 m_\rho^2} 2F_A^2 \left[ 1 - \frac{m_\pi^2}{2m_A^2} \right] \frac{1}{m_\pi^2 - m_A^2} - \alpha_\pi^0(0) \\ &\simeq +2.4 \cdot 10^{-4} \text{ fm}^3 \end{aligned} \quad (23)$$

for  $F_A = 1$ . This result is to be compared with  $\alpha_\pi^+ = 2.7 \cdot 10^{-4} \text{ fm}^3$  following from chiral perturbation theory [13], and the data  $\alpha_\pi^+(\text{exp}) = (2.2 \pm 1.6) \cdot 10^{-4} \text{ fm}^3$  [14].



## 5. Conclusions

In the master formula approach to chiral symmetry breaking, the two-photon fusion process is expressed in terms of two vacuum correlation functions. One of the correlation function drops in the chiral limit. These correlation functions are amenable to lattice estimates. In this paper they were saturated by low mass excitations at tree level. The results for the charged fusion process are dominated by the Born term, and overall insensitive to the low mass excitations. In the chargeless channel, our analysis shows a clear contribution from a broad scalar-isoscalar resonance with  $m_\sigma \sim 500\text{MeV}$  and  $\Gamma_\sigma \sim 550\text{MeV}$ , much like the one seen in  $\pi\pi$  scattering for the scalar-isoscalar channel. The pion polarizabilities are also found in fair agreement with the data. Our results compare favorably with the two-loop analysis and results from dispersion theory. In fact, our approximations are amenable to specific weights in the spectral analysis of the correlation functions. From this point of view our results are similar in spirit to the dispersion analysis with full compliance with the underlying Ward identities. Also they provide simple insights to two correlation functions that can be compared with future lattice simulations.

## Acknowledgements

We would like to thank Dr. Hidenaga Yamagishi for discussions. This work was supported in part by US DOE grant DE-FG-88ER40388.

## References

- [1] J. Bijnens and F. Cornet, Nucl. Phys. **B296** (1988) 557.
- [2] J.F. Donoghue, B.R. Holstein and Y.C. Lin, Phys. Rev. **D37** (1988) 2423.
- [3] The Crystal Ball Collaboration (H. Marsiske et al.), Phys. Rev. **D41** (1990) 3324.
- [4] S. Belluci, J. Gasser and M.E. Sainio, Nucl. Phys. **B423** (1994) 80.
- [5] D. Morgand and M.R. Pennington, Phys. Lett. **B272** (1991) 134;  
T.N. Truong, Phys. Lett. **B313** (1993) 221.
- [6] J.F. Donoghue and B.R. Holstein, Phys. Rev. **D48** (1993) 137.
- [7] P. Ko, Phys. Rev. **D41**, 1531 (1990).
- [8] H. Yamagishi and I. Zahed, A Master Formula Approach to Chiral Symmetry Breaking, SUNY-NTG-94-57; Ann. Phys. in Print.
- [9] I. Zahed and G.E. Brown, Phys. Rep. **C142** (1986) 1.  
Ulf-G. Meißner, Phys. Rep. **C161** (1988) 213.
- [10] G. Ecker et al. *Nucl. Phys.* **B321** (1989) 311.
- [11] E. Shuryak, Acta Phys. Pol. **25** (1994) 115.
- [12] J. Steele, H. Yamagishi, and I. Zahed, Master Formula Approach to Chiral Symmetry Breaking:  $\pi\pi$ -scattering, SUNY-NTG-95-14; Submitted to Nucl. Phys. **B**.
- [13] B.R. Holstein, Comm. Nucl. Part. Phys. **19** (1990) 239, and references therein.
- [14] The Mark II Collaboration (J. Boyer et al.), Phys. Rev. **D42** (1990) 1350.  
D. Babusci *et al.*, Phys. Lett. **B227** (1992) 158.
- [15] A.E. Kaloshin and V.V. Serebryakov, Phys. Lett **B278** (1992) 198.

## Figure captions

**Figure 1:** Dominant contributions to the vacuum correlators in the process  $\gamma\gamma \rightarrow \pi\pi$  as given by Eq. (2). The solid V-lines refer to the isovector vector-current  $\mathbf{V}$ , the solid A-lines refers to the one-pion reduced isovector axial-current  $\mathbf{j}_A$ , and the solid S-line refers to the scalar current triggered by  $\hat{\sigma}$ . The wiggly lines indicate incoming photons, and the dashed lines outgoing pions. The crossed contributions are understood.

**Figure 2:** Subleading diagrams stemming from the vacuum correlator  $\mathbf{j}\mathbf{j}\mathbf{V}\mathbf{V}$  featuring  $\pi A_1$ -mixing.

**Figure 3:** The  $\gamma\gamma \rightarrow \pi^0\pi^0$  cross section  $\sigma$  ( $|\cos\theta| \leq 0.8$ ) as a function of the center-of-mass energy  $\mathcal{E}_{\gamma\gamma} = \sqrt{s}$  with the data from the Crystal Ball experiment [3]. Our best fit (solid line) as compared to the two-loop result [4] (dashed line).

**Figure 4:** The  $\gamma\gamma \rightarrow \pi^+\pi^-$  process as a function of  $\mathcal{E}_{\gamma\gamma} = \sqrt{s}$ . Our cross section (solid line) versus one-loop  $\chi$ PT (dashed) and tree (dot-dashed) [1, 2] results. Data points are taken from Mark II experiment [14].

**Figure 5:** The Compton scattering  $\gamma\pi^\pm \rightarrow \gamma\pi^\pm$  cross section as a function of the CM energy  $\mathcal{E}_{\gamma\pi} = \sqrt{s}$ . Our result (solid line) as compared to the two (dashed) and one-loop (dot-dashed)  $\chi$ PT calculations [4].

FIGURES

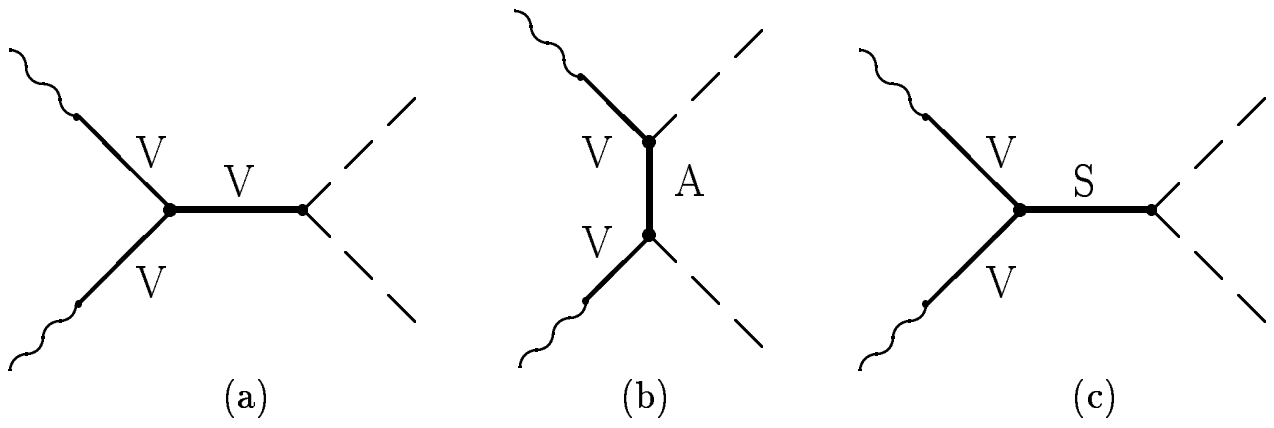


*Figure 1.*

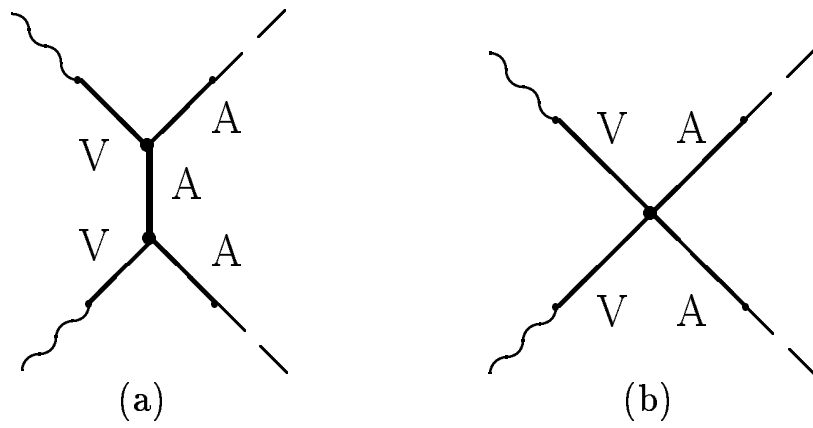


*Figure 2.*

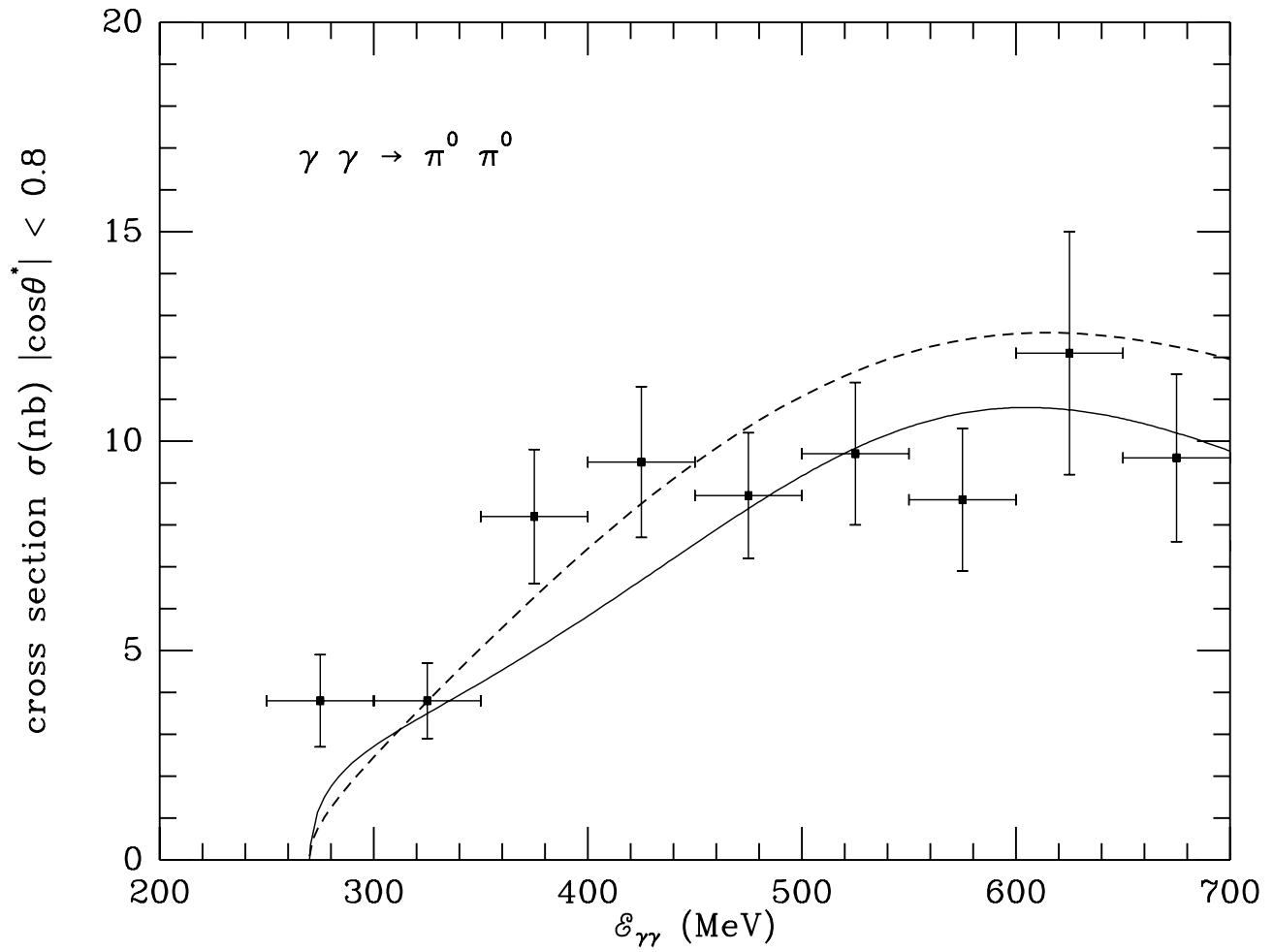


Figure 3.

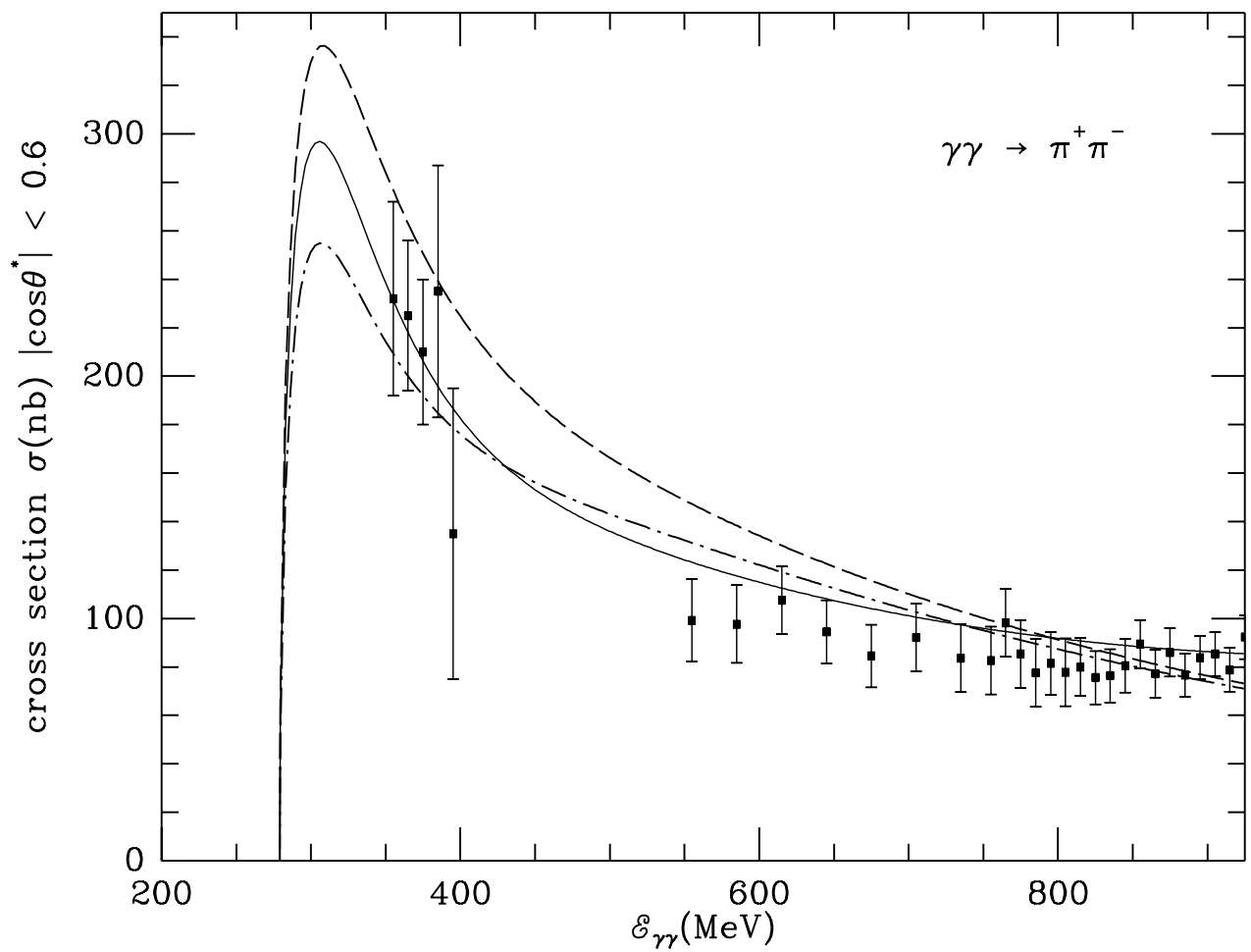


Figure 4.

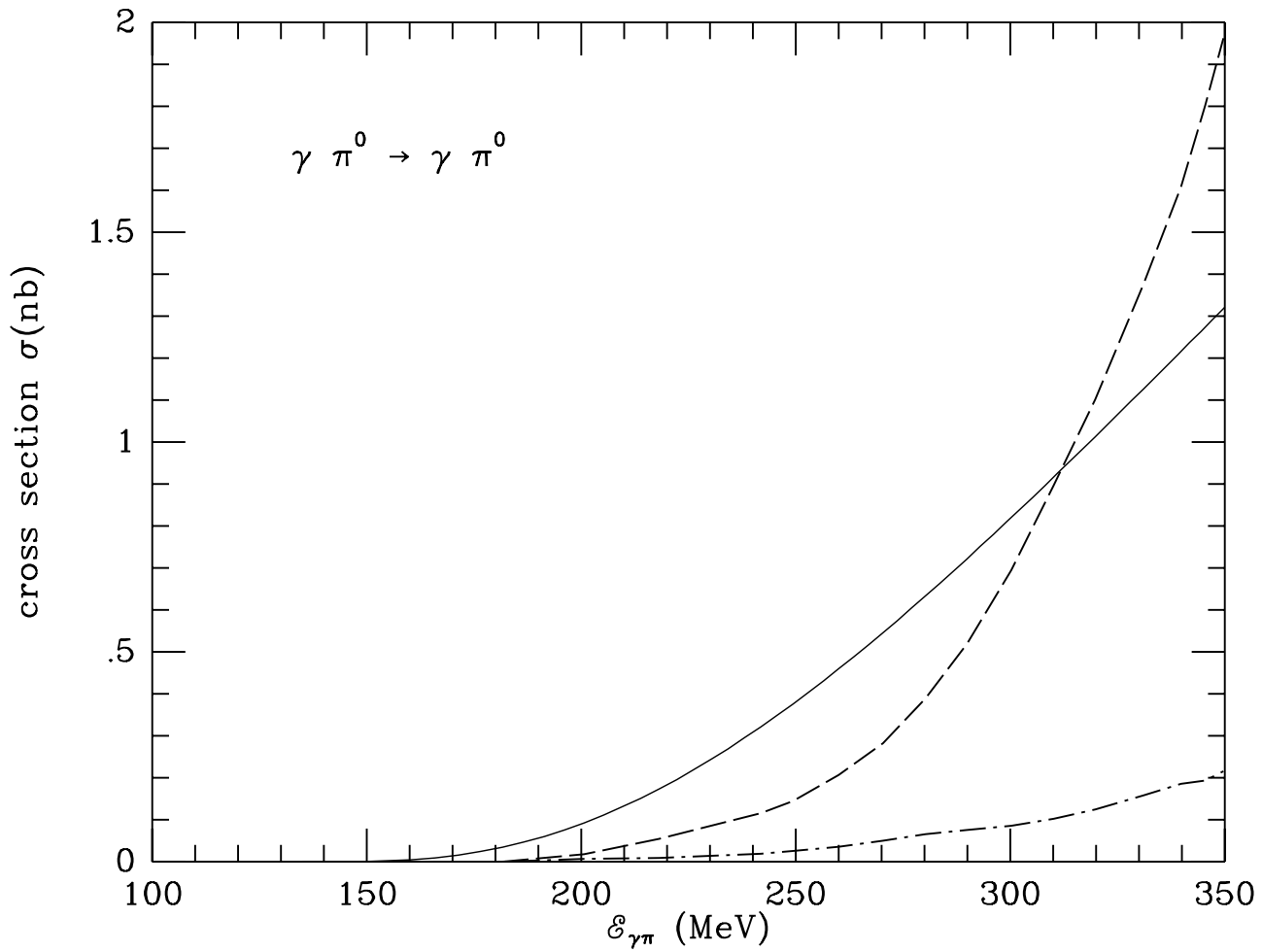


Figure 5.